

UNCLASSIFIED

AD 286 254

*Reproduced
by the*

ARMED SERVICES TECHNICAL INFORMATION AGENCY
ARLINGTON HALL STATION
ARLINGTON 12, VIRGINIA



UNCLASSIFIED

NOTICE: When government or other drawings, specifications or other data are used for any purpose other than in connection with a definitely related government procurement operation, the U. S. Government thereby incurs no responsibility, nor any obligation whatsoever; and the fact that the Government may have formulated, furnished, or in any way supplied the said drawings, specifications, or other data is not to be regarded by implication or otherwise as in any manner licensing the holder or any other person or corporation, or conveying any rights or permission to manufacture, use or sell any patented invention that may in any way be related thereto.

286 254

63-1-2

Technical Report SELWS-M-4
October 1962

286254

CATALOGED BY ASTIA
AS AD 110

PERFORMANCE CHARACTERISTICS OF METEOROLOGICAL
ROCKET WIND AND TEMPERATURE SENSORS

PREPARED BY

MISSILE METEOROLOGY DIVISION

U. S. ARMY
ELECTRONICS RESEARCH AND DEVELOPMENT ACTIVITY
WHITE SANDS MISSILE RANGE
NEW MEXICO

U. S. ARMY ELECTRONICS RESEARCH AND DEVELOPMENT ACTIVITY

**WILLIAM G. SKINNER
COLONEL, SIGNAL CORPS
COMMANDING**

**PERFORMANCE CHARACTERISTICS OF METEOROLOGICAL
ROCKET WIND AND TEMPERATURE SENSORS**

by

**Norman J. Beyers
U. S. Army Electronics Research and Development Activity**

**Otto W. Thiele
U. S. Army Electronics Research and Development Activity**

and

**Norman K. Wagner
The University of Texas**

SELWS-M-4

October 1962

MISSILE METEOROLOGY DIVISION

**WHITE SANDS MISSILE RANGE
NEW MEXICO**

ABSTRACT

Numerous meteorological rocket firings have been conducted at missile ranges to obtain atmospheric data in support of missile tests, and the Meteorological Rocket Network has resulted in coordinated firings designed to provide a synoptic picture of the high atmosphere. Rocket-borne inertial systems consisting of radar chaff and metalized parachutes have been utilized to determine wind flow in the altitude range from 50,000 to 250,000 feet. Fall velocities, parachute oscillations, chaff dispersion, and wind sensor lag times have been examined with radar and radiosonde ground equipment. Some of the problems involved in the temperature measuring system (Gamma) are also treated with respect to time constant, radiative effects, compressional and nosecone heating, and internal heating. Typical wind and temperature profiles are presented along with an application of the temperature profile to speed-of-sound and density calculations.

CONTENTS

	PAGE
ABSTRACT	iii
INTRODUCTION	1
PARACHUTE WIND SENSORS	2
RADAR CHAFF WIND SENSORS	9
WIND MEASUREMENT ERRORS	12
THE TEMPERATURE SENSING SYSTEM	14
RADIATIVE AND COMPRESSIONAL HEATING ERROR	15
ADDITIONAL SOURCES OF ERROR	21
APPLICATIONS AND CONCLUSIONS	23
REFERENCES	29

FIGURES

1. The Gentex 15-Foot Diameter Parachute Used With the Arcas Rocket	3
2. Fall Velocity Versus Altitude of Rocket Winds Sensors at White Sands Missile Range, New Mexico	5
3. GMD-1 Signal Strength Versus Time Records	7
4. AN/FPS-16 Radar Track of a 15-Foot Arcas Parachute	8
5. Foil and Cylindrical Chaff	11
6. Wind Shear Error Versus Altitude for the 15-Foot Arcas Parachute	13
7. Time Constant of the Arcas Rocketsonde Thermistor	16
8. Combined Compressional Heating and Radiative Temperature Error of the Arcas Rocketsonde Thermistor	22
9. Indicated Temperature and Temperature Corrected for Compressional Heating	24
10. Power Dissipation of Gamma and Associated Temperature Rise at 8mm Pressure with Krylon Coated Bead Thermistor	25

	PAGE
11. Typical Rocketsonde-Raob Profile	26
12. Density and Speed of Sound Profiles Derived From Rocketsonde Data	28

TABLES

I. Wind Response Characteristics of the 15-Foot Arcas Parachute---	10
II. Values of Height Dependent Parameters	17
III. Temperature Correction Factor to be Added to Observed Tempera- ture for Daytime and Nighttime Soundings	17

INTRODUCTION

Since the initiation of the Meteorological Rocket Network (Webb et al 1961) in October 1959, appreciable data have been obtained in the altitude range from 50,000 to 250,000 feet. A majority of the data have consisted of wind measurements made by radar tracking of passive wind sensors including radar-reflective chaff and metalized parachutes. Many temperature soundings have also been accumulated and applied to pressure and density calculations.

The meteorological rocket vehicles, Arcas and Loki, have been described adequately elsewhere (Jenkins et al 1960) and the discussion here will be limited mainly to the sensor characteristics and measuring techniques. Although data presented here are primarily from operations at White Sands Missile Range, New Mexico, the flight equipment and ground instrumentation are basic and typical of other Meteorological Rocket Network Stations.

Chaff need be subjected only to the considerations involving its application as a wind sensor and, while these are complex in themselves, the parachute considerations are compounded by the dual responsibility of serving both as a wind sensor and as a carrier for the temperature instrumentation. Hence, parachute characteristics such as oscillation and fall velocity are examined first with respect to the effects on the wind sensing ability and then with respect to the effects on the temperature system. It is indeed fortunate for design purposes that most of the characteristics that are desirable for a wind sensor are also desirable for the temperature sensing system. There is, however, at least one important conflict involving the minimum payload weight necessitated by temperature instrumentation suspended on the parachute resulting in greater than optimum fall velocities.

Wind speed and direction are calculated from the horizontal displacement per unit time of the parachute or chaff as determined by radar. Basically, the reduction technique is similar to the other standard wind measuring systems (pibals and rawins) in that averages of horizontal movement are determined and assigned to the mean altitude over a given time period. There are, however, problems inherent in the rocket measuring system which are not found in the other standard methods. These include possible errors introduced through excessive fall velocities of both parachutes and chaff, chaff dispersion, and parachute slip and glide. Of course, instrumental precision of the tracking equipment is a consideration common to all methods and must be examined. There is a basic similarity between the temperature measuring technique of the rocket-borne system and the standard radiosonde technique. While most of the same factors such as the time constant, solar radiation effect, internal heating, and compressional heating are present in both systems, the effects vary considerably, because of the altitude ranges over which they are applied.

PARACHUTE WIND SENSORS

Primary emphasis in this discussion is placed on the Centex 15-foot metallic-coated, baseball elliptical parachute (Figure 1), used in conjunction with the Arcas meteorological sounding rocket, because of the larger amount of data and experience acquired with this type of parachute. However, an 8-foot metalized mylar parachute has been used extensively with the Loki-Dart Phase I system. The parachute with a 1-pound inert weight attached is packaged in the 1-3/8 inch dart. An acceleration actuated pyrotechnic or mechanical time fuse fires an expelling charge at a peak altitude of 120,000 to 160,000 feet.

Expelling the 15-foot parachutes from Arcas rockets without damage to the instrumentation or the parachute is something of a problem, primarily because of the inability to control the expulsion time, peak altitude, and rocket attitude. The peak altitudes of the rockets vary by as much as 30,000 feet; also, the pyrotechnic time fuses vary by as much as 15 per cent. If expulsion occurs before peak and if the rocket is stable, it is possible for the rocket body, having less drag, to overtake the parachute and either damage or foul it. Furthermore, there is the possibility, either before or after peak, of the instrumentation package falling back into the parachute because of differential drag. The highest altitudes are obtained when the rocket is most stable, and it has been under these circumstances that most of the deployment problems have occurred. A certain amount of pitch and yaw are usually characteristic of a free-flight rocket, and this feature is depended upon to impart some velocity away from the trajectory upon expulsion, thereby preventing subsequent collision of the parachute and rocket body. There have been instances when the instrumentation had apparently fallen into the parachute, then fell clear, only temporarily fouling the parachute. In some of these instances the thermistor lead wires were broken.

Thus far, expulsion and subsequent deployment characteristics of the parachutes at high altitudes have been difficult to evaluate since only a limited amount of applicable data is available from radar tracks and instrumentation effects; however, the overall reliability of normal deployment is approximately 80 per cent with more than half of the remaining 20 per cent producing some usable data.

There is evidence that parachutes stream, slip, or do not fully deploy at altitudes above 220,000 feet. This evidence is based on the fact that the observed fall rates are considerably greater than anticipated from theoretical calculations and that during this period the parachute is not a very good radar reflective target. The variously modified SCR-584 and M-33 radars do not have the capability of tracking the entire trajectory and have, therefore, some difficulty in acquiring the target during this period even when the range is relatively short. This acquisition problem does not occur when FPS-16 type radars are used since such radars have the capability of skin tracking Arcas rockets to payload expulsion. Thus, for the FPS-16, it is not difficult to transfer immediately to the

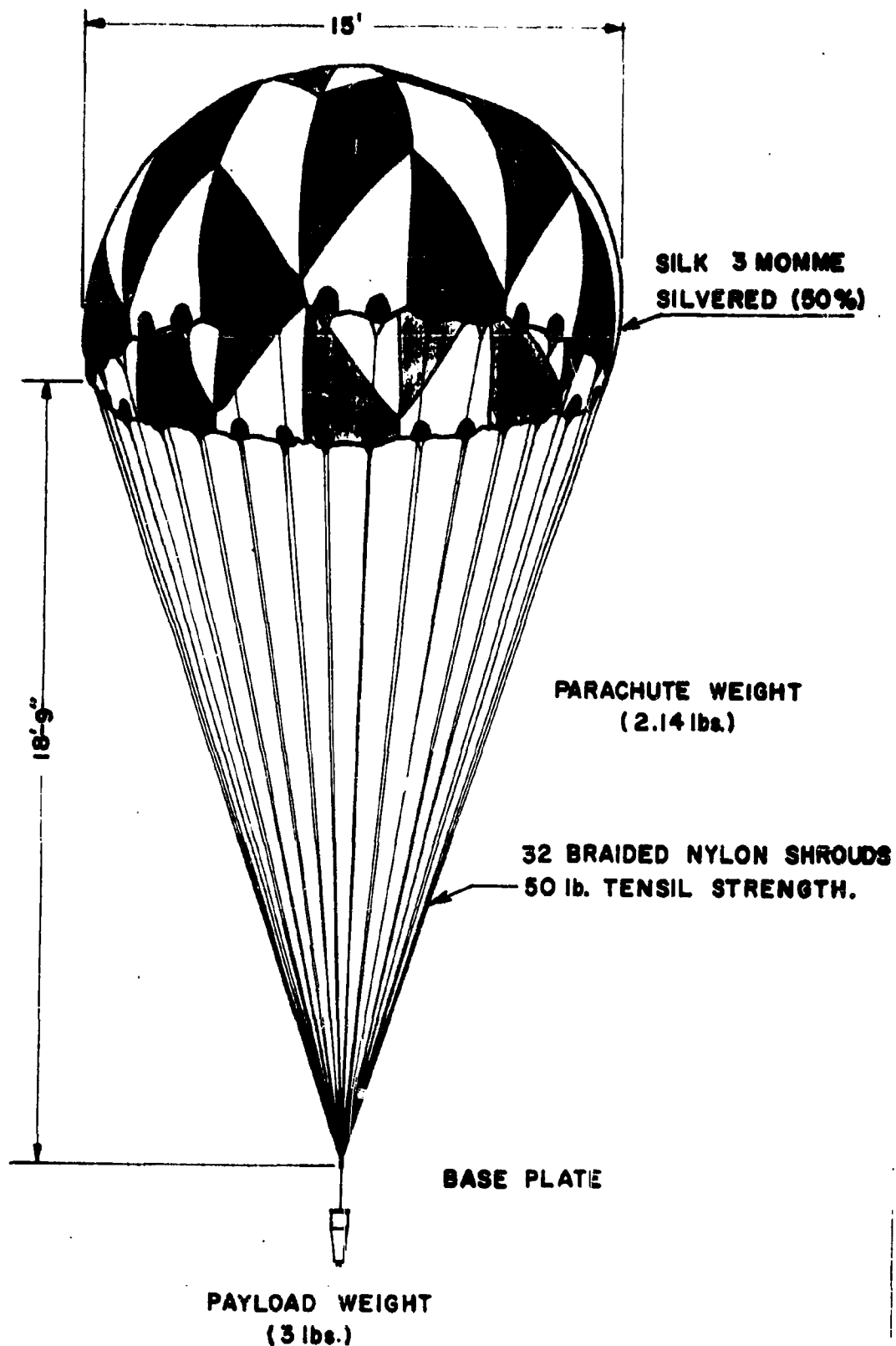


Figure 1. The Gentex 15-foot diameter parachute used with the Arcas rocket.

parachute at ejection because in almost any condition, the metalized parachute will offer a larger target than the rocket body. Unfortunately, FPS-16 type radars are not available at all of the Arcas launching sites currently in use.

There have been no deployment problems using the 8-foot metalized mylar parachute with a 1-pound weight at Loki Phase I altitudes of 120,000 to 160,000 feet. All evidence obtained using the 8-foot parachute indicates that full deployment occurs almost immediately after expulsion, providing an excellent radar target.

The fall velocity of the Arcas 15-foot parachute is illustrated in Figure 2. The data below 220,000 feet represent the mode and range of over 50 cases irrespective of peak altitude. The range of fall velocities is, no doubt, mainly a function of the expulsion altitude. Above 220,000 feet the probable accuracy of the data obtained from radar plotting board graphical trajectories is ± 100 feet per second, while the probable accuracy of the values below 220,000 feet obtained in the same manner is ± 20 feet per second. The fall velocity of the 8-foot parachute is also presented in Figure 2.

The efficiency of a descending passive wind sensor is directly dependent on the fall velocity. An extremely high fall velocity will render the parachute relatively insensitive to all but the most intense wind shears while low velocities provide excellent response characteristics. However, low fall velocities introduce a problem of another nature, namely, excessive track time which can be serious because of the instrumentation and operators necessary for extended tracking purposes. For our application, an acceptable range of fall velocities is from 50 to 200 feet per second. Essentially, the vertical velocity of a passive wind sensor should not greatly exceed the horizontal velocities that are to be measured. Obviously, this condition cannot be achieved at extremely high altitudes with a parachute. Consequently, small-scale variations cannot be accurately detected in this region. A relative order of magnitude for large shears may be obtained at high altitudes, and the detection of strong winds when present at these altitudes is still of primary interest. Comparative data on actual wind shears are not available so an empirically deduced maximum acceptable fall rate cannot be determined, but theoretical studies of acceptable limits for high-altitude passive wind sensors have been made by Barr (1960), Lally and Leviton (1958), and Rapp (1960).

The Arcas parachute exhibits a very pronounced oscillation. Although radar data indicate this oscillation, the primary source of information regarding the effect is the variation of telemetry signal strength observed at the ground. The Arcas payload telemetering transmitter operates on 1680 mc using a quarter-wave stub antenna. The antenna pattern for this instrumentation indicates that the amplitude of oscillation is greater than 45 degrees and possibly as much as 90 degrees during the first two or three minutes after parachute deployment.

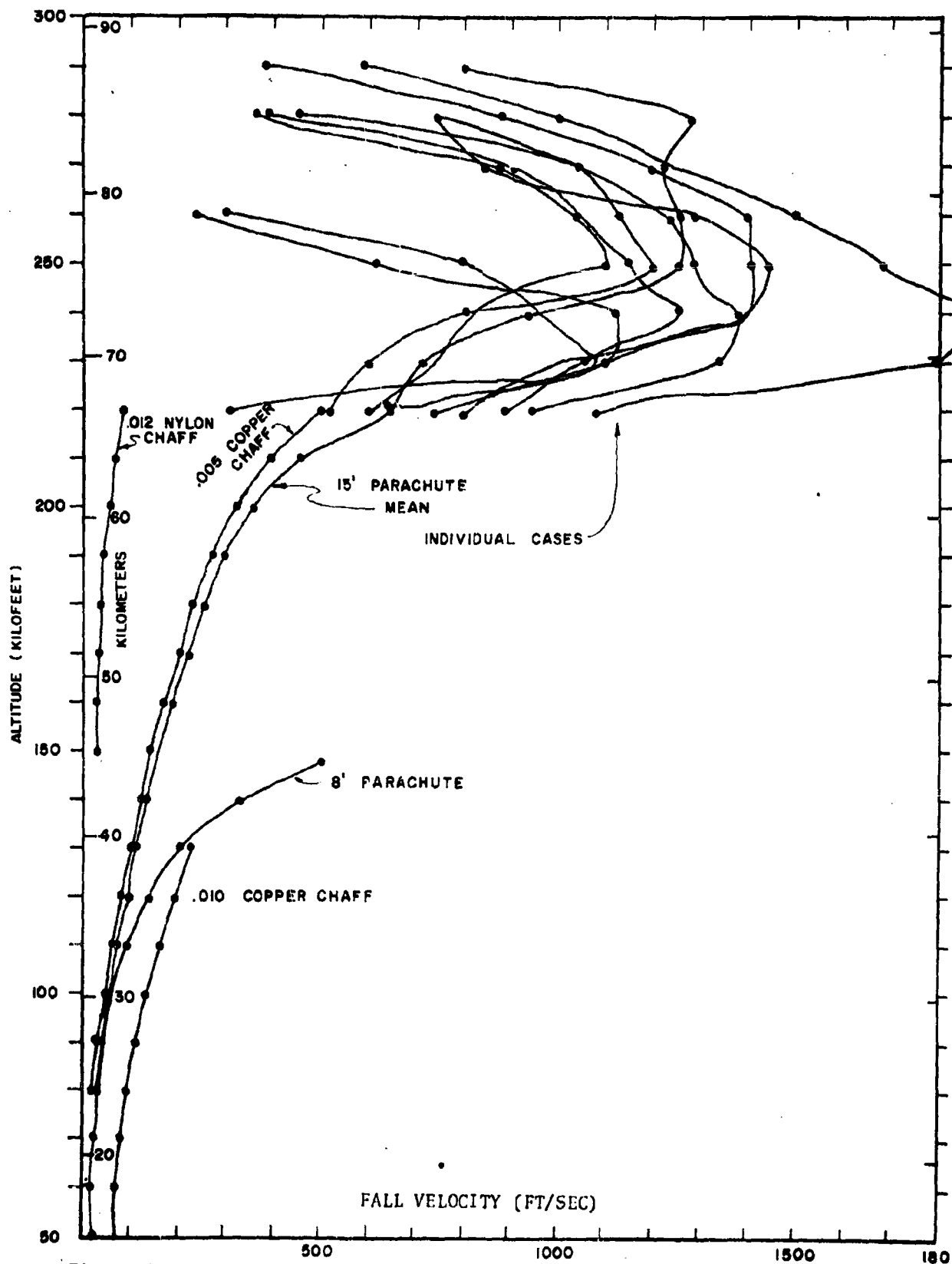


Figure 2. Fall velocity versus altitude of rocket winds sensors at White Sands Missile Range, New Mexico.

Oscillation of the parachute is clearly illustrated in Figure 3, a reproduction of representative signal strength recordings obtained from three Arcas firings.

The parachute and payload configuration may be described as very nearly representing a physical pendulum, but the performance characteristics of a simple pendulum are exhibited. During the earlier and more stable portion of the oscillation, the period of oscillation as taken from the records is approximately five seconds. The same value is obtained using the "simple pendulum" relationship

$$T_p = 2\pi\sqrt{L/g}$$

where T_p is the period of parachute oscillation, g the acceleration of gravity at altitude of oscillation, and L the effective length of the pendulum (20 feet). After several minutes, the period of oscillation gradually increases to approximately eight seconds. Since the system remains static in physical dimensions, the increase in period is attributed to increased drag and possibly a tendency toward a more circulatory oscillation. An increasing amplitude, causing a departure from simple harmonic motion, would also lengthen the period. However, the decreasing magnitude of signal strength variation does not indicate this. During the early phases of the flight, the nulls in the signal strength variation represent almost a complete loss of signal during these short intervals, but this can be tolerated with the single channel of data being received.

The effect of the oscillation on the signal level received at the GMD (assuming the GMD is located in the proximity of the launcher) is no longer apparent after about 20 to 23 minutes. The reason for this involves the antenna pattern of the flight instrument and, consequently, the geometry between flight and ground equipment. The recorded antenna pattern of the flight instrument typically contains a null along the vertical axis with lobes along the horizontal axis. Prevailing winds during the descent carry the instrument to such a horizontal distance from the ground equipment that the elevation angle from the GMD to the flight package is small. Whatever oscillation may still prevail in the parachute configuration does not overcome this geometry.

In early firings of the Arcas there was concern over the length of time the parachute might retain the horizontal velocity component it had when ejected from the rocket. This velocity retention period was termed the lag time. Figure 4 is a tracing from an actual plotting board record of an FPS-16 radar at Pacific Missile Range, California. Six cases (of which Figure 4 is typical) were examined. It was apparent from these cases that two factors combined to furnish much conclusive evidence concerning the lag time; namely, a complete "skin track" through apogee and

**GMD-1 SIGNAL STRENGTH VERSUS TIME RECORDS
 USING MODIFIED AN/AMT-4 TRANSMITTER TO SHOW PERIOD
 OF PARACHUTE OSCILLATION FOR THREE (3) ARCAS FIRED
 AT FORT CHURCHILL, CANADA.**

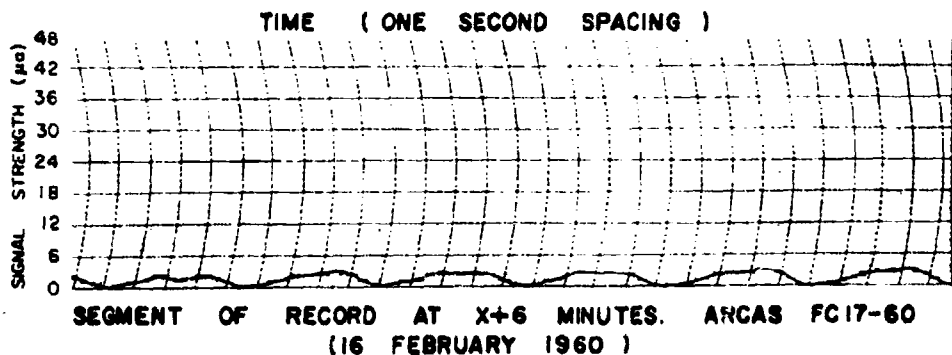
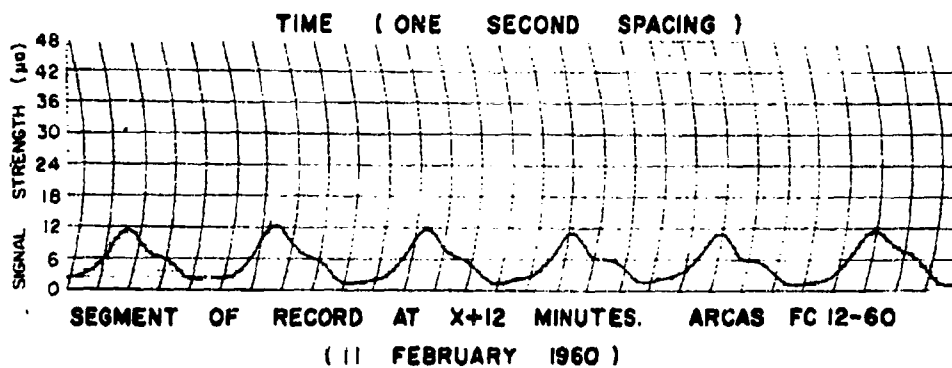
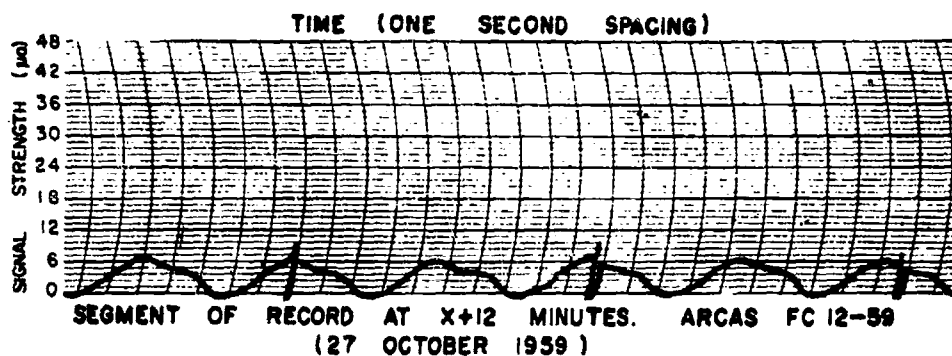
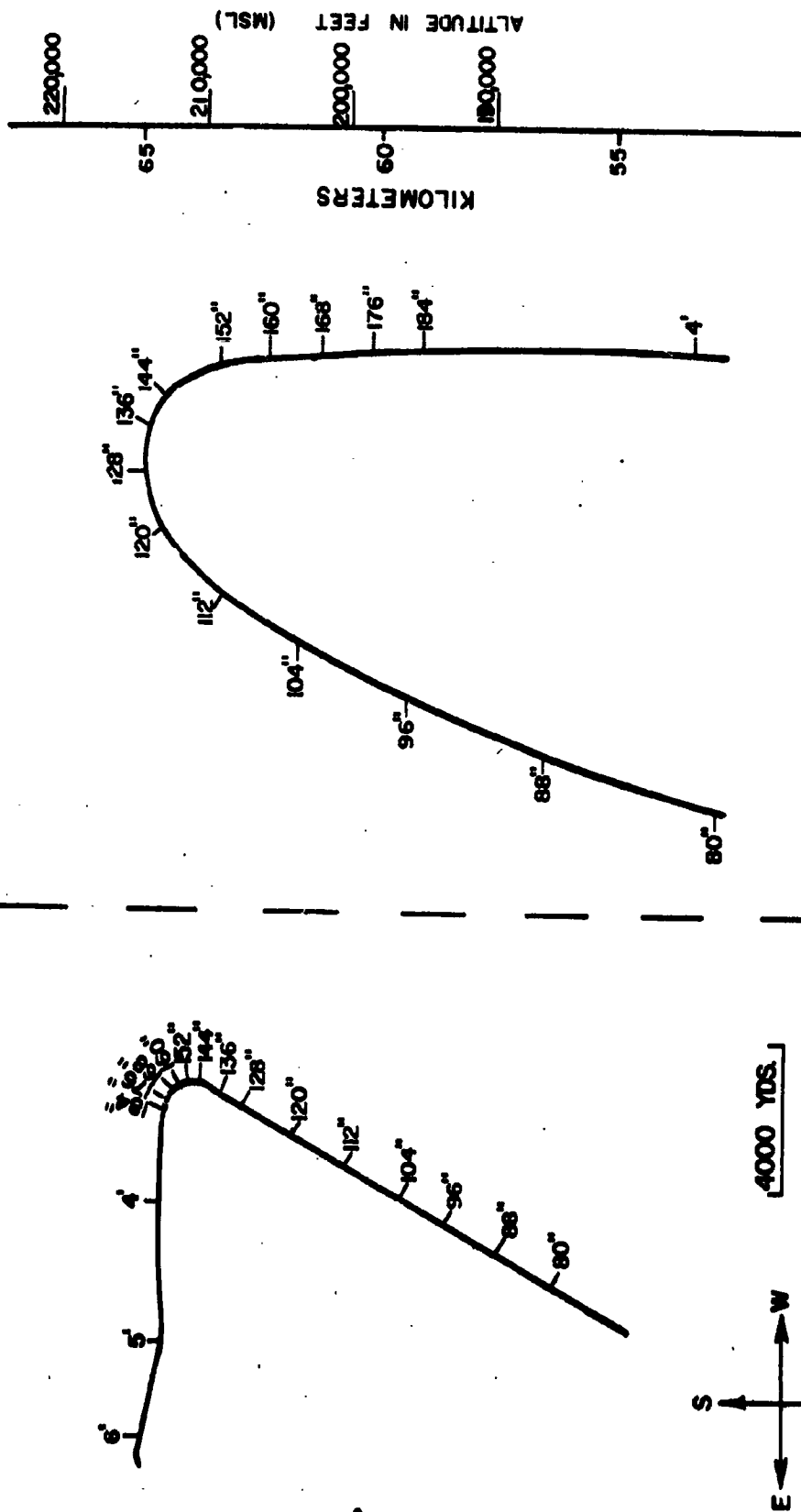


Figure 3

NOTE: Parachute ejection at 128 seconds

XY - PLOT

Z - PLOT



2 MAR 1960

Figure 4. AN/FPS-16 radar track of a 15-foot Arcas parachute.

a firing azimuth which was generally cross wind at the point of parachute expulsion.

In four of the six cases evaluated (Table I), all of the initial horizontal velocity component had disappeared within 20 seconds of the actual expulsion time. In each of the cases presented, the observed time period for total dissipation of the initial velocity component (before expulsion) represents a maximum lag; that is, it was assumed that there was no wind velocity component in the payload direction at expulsion. An examination of the case of 2 March 1960, in which the lag time was greatest, reveals the possibility that this assumption was untrue. Consequently, the lag time in this case might actually have been less than 20 seconds.

It is interesting to note in Table I that there is no apparent correlation between the lag time and the horizontal velocity component at expulsion time. Clearly then, one must know the drag characteristics of the parachute cone configuration as well as the forces acting on it during the lag period, neither of which is known for the cases presented.

RADAR CHAFF WIND SENSORS

The excessive fall velocities of parachutes at altitudes above 200,000 feet have necessitated the application of other wind sensors such as radar chaff. Two basic types of chaff, metal foil and cylindrical dipoles (Figure 5), have been used by the U. S. Army Electronics Research and Development Activity, White Sands Missile Range, New Mexico. The foil chaff used consisted of ribbons of aluminum, brass or copper while the cylindrical dipoles were of these metals or metallized nylon varying in diameter from 0.0035 to 0.012 inch. The chaff was cut to half wave length for s, c, or x band radar. Early in the meteorological rocket program at White Sands Missile Range the cylindrical dipole chaff was established as a standard and has been used almost exclusively to date; therefore, the data presented here will deal with cylindrical chaff performance characteristics. The Loki system chaff payloads average from one to three pounds and contain in excess of a million dipoles.

Chaff fall rates have been examined through analysis of radar plotting board data. The plotting board provides continuous graphical X-Y and Z-R trajectories with a standard scale factor of either 2,000 or 4,000 yards per inch. Manual time marks (accurate to within two seconds) are imposed on the trajectories at a frequency of two per minute.

Included in Figure 2 are fall velocity data for three sizes of cylindrical chaff. The .010 copper chaff was deployed from the Loki I system which peaks between 140,000 and 150,000 feet when fired at White Sands Missile Range, while the other two types depicted were carried in Loki II

Table I
WIND RESPONSE CHARACTERISTICS OF THE
15-FOOT ARCAS PARACHUTE

<u>Date</u>	<u>Lag Time</u>	<u>Horizontal Velocity Component at Expulsion Time</u>
4 Feb 60	10 secs	850 ft/sec
15 Feb 60	20 secs	700 ft/sec
16 Feb 60	<10 secs	500 ft/sec
17 Feb 60	16 secs	625 ft/sec
26 Feb 60	54 secs	560 ft/sec
2 Mar 60	40 secs	560 ft/sec

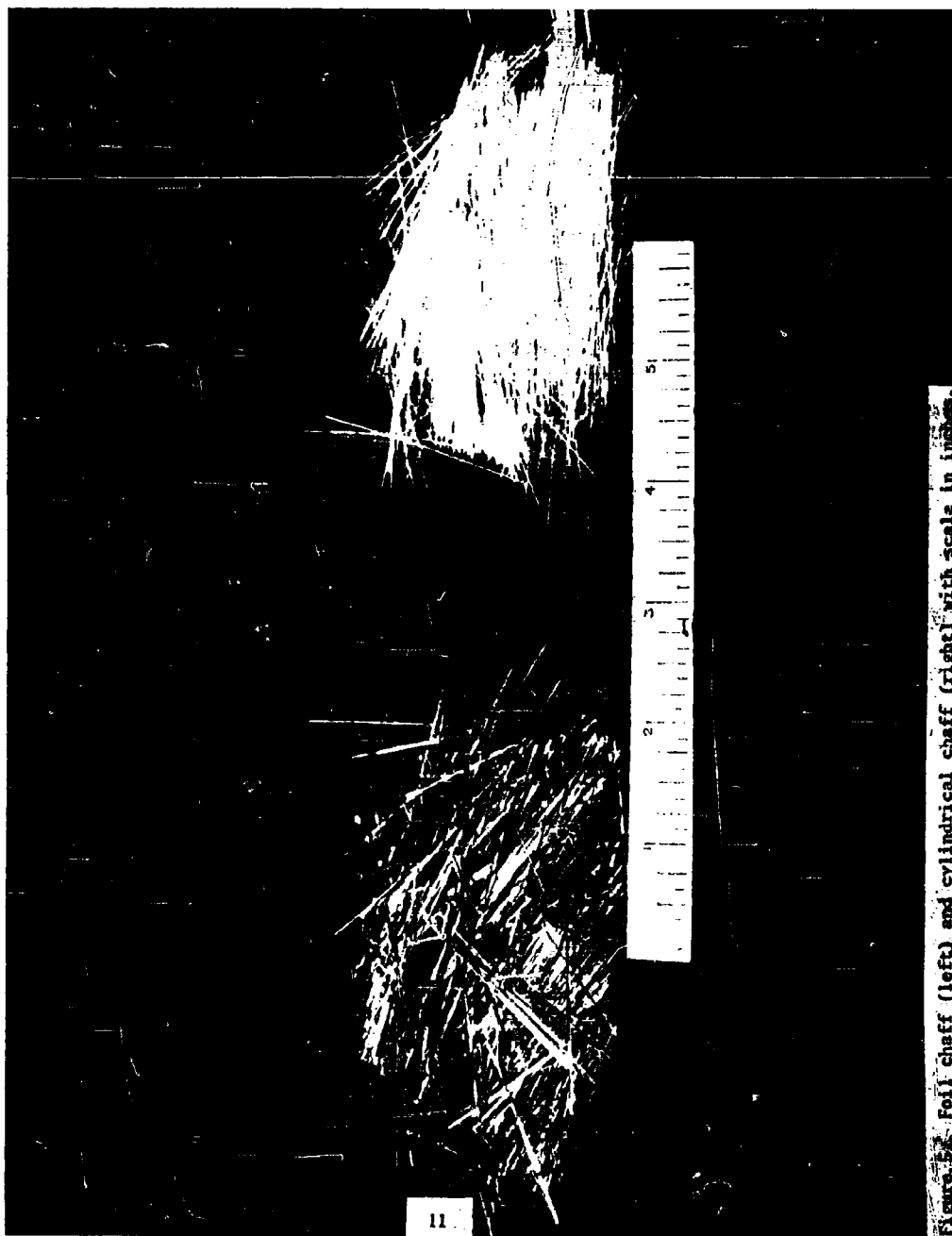


Figure 5-2. Foil chaff (left) and cylindrical chaff (right) with scale in inches.

systems which averaged 240,000 feet peak altitudes. The most obvious significant factor exhibited in Figure 2 is the range of variation in the fall velocity of the types of chaff. Above 220,000 feet only the nylon fall velocity lies in the acceptable range. The .005 copper appears desirable between 100,000 and about 180,000 feet while the .010 copper has fall velocities which are optimum between about 40,000 and 120,000 feet.

Dispersion detracts significantly from the usefulness of chaff. Two primary problems directly resulting from dispersion are signal return deterioration and tracking inaccuracies as the radar beam moves about through the chaff cloud. Radar observations of .012 cylindrical nylon chaff indicate that these chaff payloads disperse over areas of greater than 35 cubic miles within 20 minutes of chaff deployment and over 50 cubic miles in 30 minutes. Usually the radar shows two or more particular areas within the chaff cloud that reflect substantially more energy than other areas within the cloud, and one may assume that these bright spots will vary with time.

Dispersion is a function of several parameters including: fall velocity, turbulence, shear, and vertical motions, all of which may vary with time. Of the two problems resulting from dispersion, signal return deterioration is generally the lesser. A previous study (Beyers 1960) indicates an average signal deterioration rate of some 20 db per hour which is usually tolerable for adequate tracking operations.

WIND MEASUREMENT ERRORS

As stated above, the ability of a falling object to sense variations in the horizontal wind structure is a direct function of its fall velocity. Figure 6 is an application to the 15-foot Arcas parachute of the theory developed by Lally and Leviton for the Robin system, and gives an indication of the errors to be expected and corrections needed. Of course, the tracking instrumentation accuracy is another primary consideration which can lead to significant errors. Precision of radar equipment used at White Sands varies from ± 0.2 to ± 2.0 mils in angles and ± 5 to ± 15 yards in range. As a result of the random nature of most of these errors, the accuracy of mean wind speeds will surpass instantaneous velocities. Another source of error peculiar to the parachute sensor involves the slip and glide characteristics; however, comparisons by Jenkins (1962) between parachutes and other wind sensors indicate this error is relatively insignificant below 200,000 feet since it cannot be detected in standard reduction techniques.

Chaff sensor accuracy considerations are similar to those of parachutes except that the slip and glide problem is replaced by dispersion. Whereas the parachute approximates a point source target, the chaff payload soon covers miles of area and the radar beam tends to wander throughout the cloud. Significant tracking improvement can be effected with radars utilizing "A" or "J" scopes by a manual range track. Since the operator has a visual monitor of the target area cross section, he can easily keep the range gate in the approximate center.

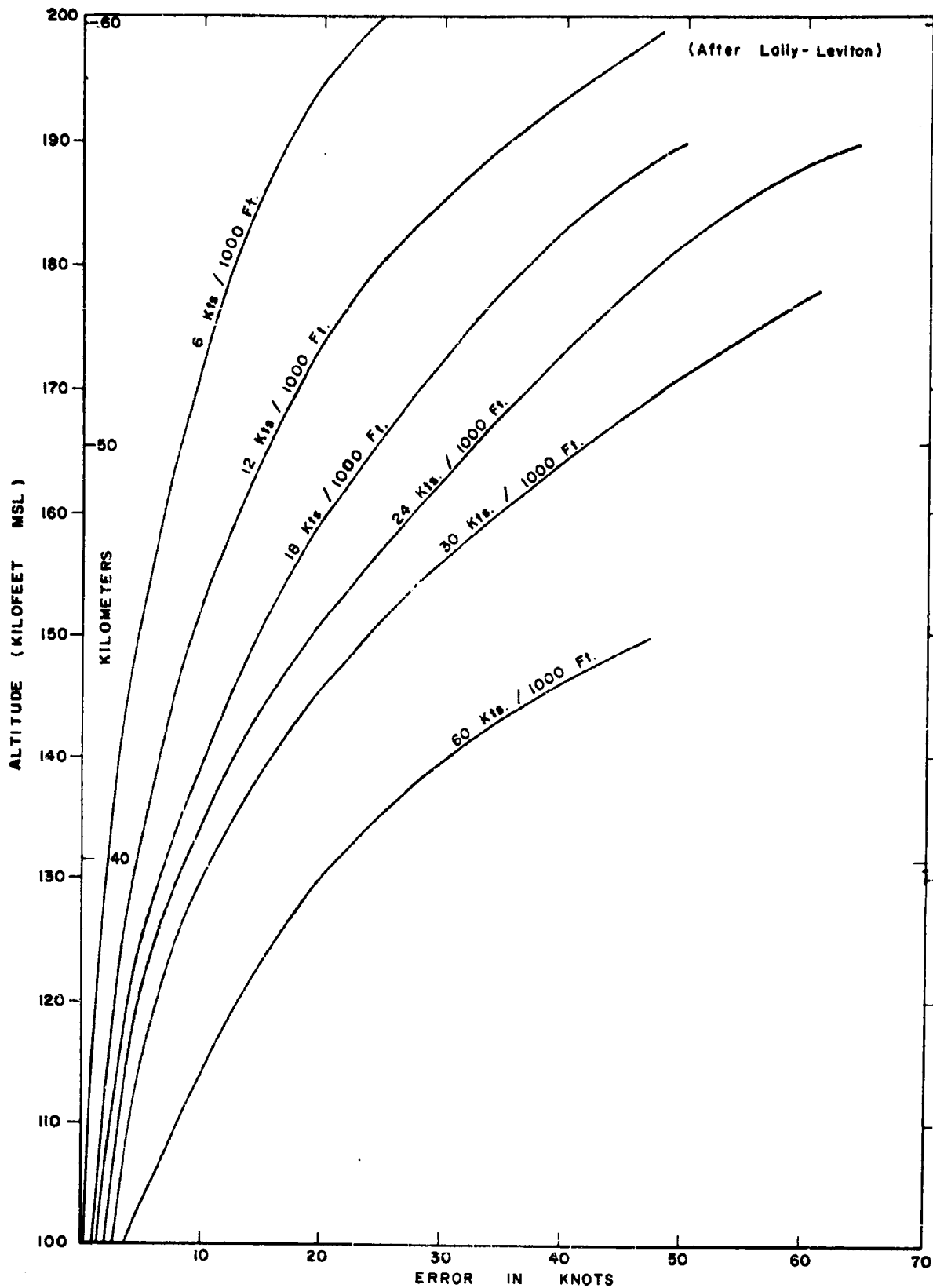


Figure 6. Wind shear error versus altitude for the 15-foot Arcas parachute.

However, it does not appear feasible to use a manual mode in azimuth and elevation since only by scanning the cloud by moving the antenna can centering be accomplished.

THE TEMPERATURE SENSING SYSTEM

The temperature sensing flight unit being used by the U. S. Army Electronics Research and Development Activity has been described in detail (Clark 1961) and only a brief description will be given here.

Basically, the flight unit consists of a 10-mil ceramic bead thermistor whose resistance controls the repetition rate of a blocking oscillator used to modulate a 1680 mc transmitter. The flight unit is suspended on the Arcas parachute with the thermistor mounted on the extreme end of the downward pointing transmitter. Standard AN/GMD-1 radiosonde ground equipment completes the system.

The temperature sensing element in current use in the Meteorological Rocket Network is a glass-coated, nearly spherical bead thermistor (Victory Engineering Corporation VECO 43A6) which has a diameter of approximately ten mils and one-mil platinum-iridium lead wires. The thermistor is given a very thin coating of white Krylon, resulting in a short-wave absorptivity of approximately 0.2 and a long-wave absorptivity of nearly 1.0. The element, associated electronic equipment, and a parachute are carried aloft by an Arcas rocket from which they are expelled near maximum altitude. Temperature measurements are taken during the descent portion of the flight. The temperature sensor is mounted such that air will come into contact with the thermistor before reaching any other portion of the instrument package. As a result of having the instrument package and parachute above the thermistor during descent, and because of the pendulum motion of the parachute, one would expect the thermistor to be exposed intermittently to direct solar radiation.

As the thermistor is exposed to the atmosphere from approximately 80 kilometers to the earth's surface, it responds to a convective and radiational environment in a way that currently defies complete theoretical description. The following sections of this article will, of necessity, make certain restrictive assumptions. However, in all cases they are reasonable assumptions, and consequently, the final results of the analysis are thought to be significant.

The convective time constant of a thermometer is defined by the expression

$$\lambda = C/hA \quad (1)$$

where C is the heat capacity of the thermometer (assumed to be 8.03×10^{-6} cal/°C), h is the convective heat transfer coefficient and A is the surface area of the thermometer. The solution of equation (1) is usually straightforward; that is, the heat capacity and size of a particular thermometer are generally constant and the heat transfer coefficient can be evaluated by standard techniques. This is true for the rocketsonde thermistor as long as we keep in mind that near the top of the sounding the sensing element is exposed to an environment

where the mean-free-path of the air molecules is large compared to the size of the thermistor. When the lower portion of the sounding is reached, the mean-free-path becomes much smaller than the size of the thermistor. This means that the thermistor will be passing from the free-molecular flow regime near the top of the sounding, through the slip-flow regime in the middle altitudes, and down to the continuous flow regime at the bottom portion of the sounding. The convective heat transfer coefficient which appears in equation (1) changes for each flow regime. Expressions for the heat transfer coefficient in each of these flow regimes for a sphere can be found in most recent texts on heat transfer (see for example Eckert and Drake, 1959).

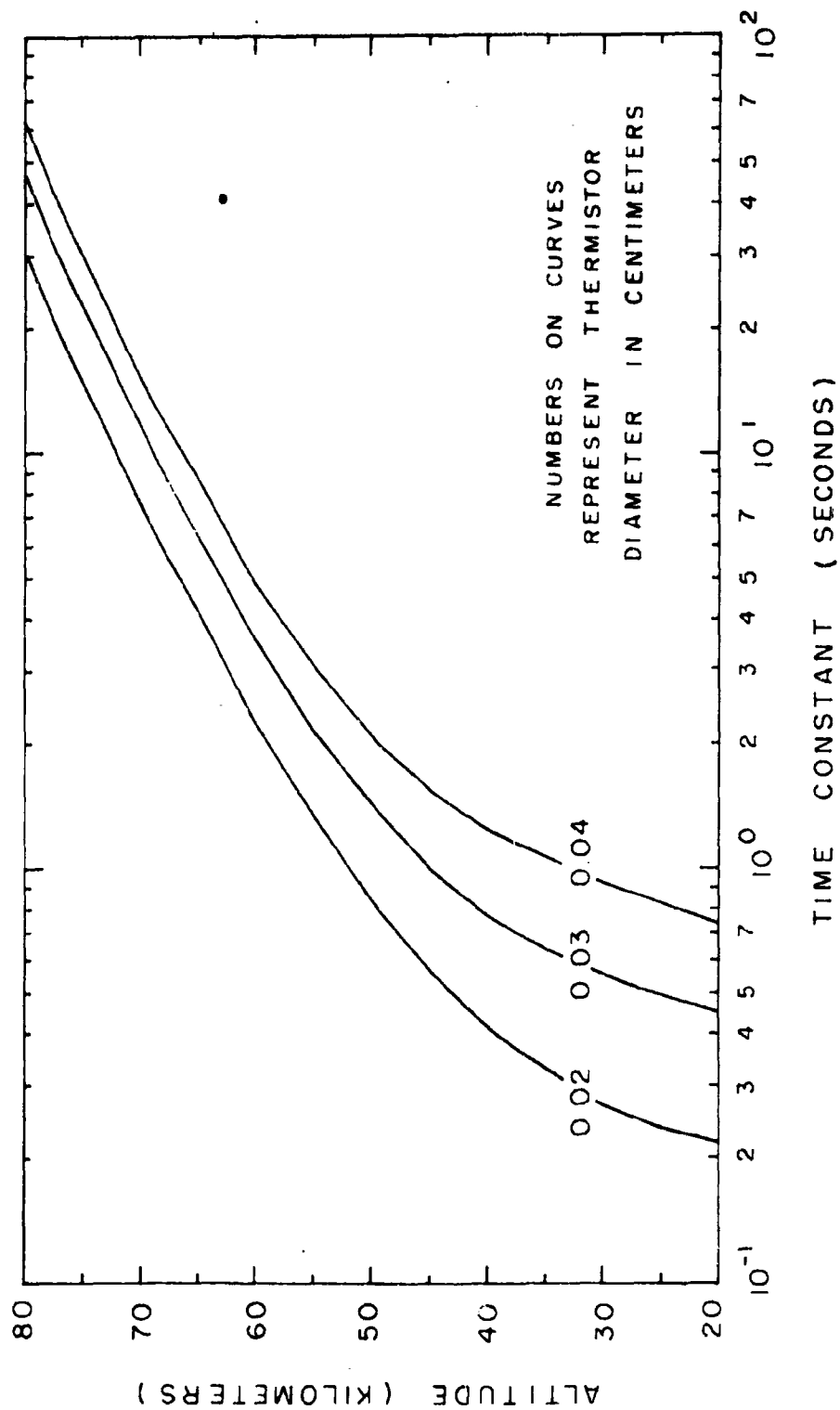
One additional piece of information which is needed before the time constant can be evaluated is the ventilating speed of the thermistor. Direct observations of the parachute fall speed by radar at the White Sands Missile Range were plotted in the height interval from approximately 30 km to 65 km. A second order polynomial was fit by least squares techniques and the resulting equation used for extrapolation down to 20 km and up to 80 km. The resulting fall speed V is shown in Table II and is assumed equivalent to the ventilation speed.

The time constant was computed for three different diameters as shown in Figure 7. The appropriate values for a diameter 0.032 cm can be obtained to a sufficient degree of accuracy by linear interpolation between the 0.03 cm and 0.04 cm curves. We find that the time constant changes by approximately two orders of magnitude over the 20 km to 80 km interval (see Table II); from 0.51 sec at 20 km to 50 sec at 80 km. A more detailed description of the computational procedure, along with an error analysis may be found in a recent article by Wagner (1961).

RADIATIVE AND COMPRESSIONAL HEATING ERROR

In addition to the quantities previously defined the following symbols will be used in this development:

T_{fe}	temperature of the far or undisturbed atmospheric environment of the thermistor, given approximately by the 1959 ARDC standard atmosphere
T_{ne}	temperature of the near atmospheric environment of the thermistor, given by an algebraic sum of T_{fe} and the temperature rise resulting from compressional-frictional heating effects
a	solar absorptivity of the thermistor
J	flux of short wave (solar) radiation reaching the thermistor
T_{be}	effective blackbody radiating temperature of the environment below the thermistor



VARIATION OF TIME CONSTANT WITH HEIGHT FOR SPHERICAL THERMISTORS

Figure 7. Time constant of the Arcas rocketsonde thermistor.

TABLE II Values of Height Dependent Parameters Used in the Solution of Equations (5) and (7)

Height (km)	T _{fe} (°K)	V (m/sec)	T _{ne} (°K)	λ (sec)	T _{be} (°K)	T _{ae} (°K)	T _{ai} (°K)
20	216.7	6	216.7	.51	253	111	219
23	216.7	8	216.7	.54	250	103	220
26	221.3	10	221.3	.58	248	96	230
29	230.6	12	230.7	.62	247	90	243
32	239.9	16	240.0	.68	247	85	254
35	249.1	21	249.3	.75	246	80	265
38	258.4	26	258.7	.84	246	76	275
41	267.7	34	268.2	.94	246	72	280
44	277.0	42	277.7	1.10	245	68	283
47	282.7	53	283.8	1.31	245	64	284
50	282.7	62	284.2	1.61	245	60	284
53	282.7	80	285.3	2.05	245	57	285
56	275.3	99	279.2	2.7	244	54	286
59	262.5	125	268.7	3.6	244	51	287
62	249.5	148	258.3	5.0	244	48	288
65	236.6	176	249.0	7.0	244	45	288
68	223.6	209	241.0	10.0	244	42	288
71	210.8	246	235.0	15.0	243	39	288
74	197.8	291	231.6	22.0	243	36	288
77	184.9	344	232.3	32.5	243	33	288
80	172.0	398	235.4	50.0	243	30	288

TABLE III Temperature Correction Factor to be Added to Observed Temperature for Daytime and Nighttime Soundings

<u>Height</u>		<u>Daytime</u>	<u>Nighttime</u>
KM	K-FT	(a = 0.1) °C	(a = 0.0) °C
	Below 30 kilometer	no correction is necessary	
38	124.6	0	+1
41	134.5	+1	+1
44	144.3	+1	+1
47	154.1	+1	+2
50	164.0	+1	+2
53	173.8	+1	+2
56	183.7	0	+1
59	193.5	-2	-1
62	203.4	-5	-4
65	213.3	-10	-7
68	223.1	-16	-12
71	233.0	-24	-19

T_{ae}	effective blackbody radiating temperature of the atmospheric and space environment above the thermistor
T_{ai}	effective blackbody radiating temperature of the instrument package above the thermistor
σ	Stefan-Boltzmann constant
T	temperature of the thermistor
t	time
$\frac{d}{dt}$	time differential operator (total derivative)
Q	heat transferred by radiation
H	heat transferred by convection
V	ventilation speed of the thermistor, assumed equivalent to the fall speed of the parachute
c_p	specific heat capacity of air at constant pressure.

If it is assumed that radiation and convection are the only heat transfer processes of importance for the temperature sensor, we may express the general heat transfer equation for the bead thermistor as

$$C(dT/dt) = Q + H. \quad (2)$$

The thermistor is attempting to reach convective equilibrium with its near environment, thus the convective heat transfer term may be expressed as

$$H = (T_{ne} - T) (C/\lambda). \quad (3)$$

The heat transferred by radiation will be considered as composed of direct and indirect solar radiation, infrared radiation from the environment below and above the thermistor, and infrared radiation from the element. The long-wave radiation from the environment above the sensor will come in part from the instrument package with the remainder from the atmospheric and space environment.

The Arcas instrument package subtends an angle of approximately 54 degrees from the center of the thermistor. One is thus able to determine that approximately 12 per cent of the upper half of the thermistor is exposed to infrared radiation from the instrument package, while the remaining 88 per cent is exposed to long-wave radiation from the atmosphere and space.

If we assume that the sensing element is a blackbody absorber and emitter of infrared radiation, we may write

$$Q = \frac{JA_a}{4} + \sigma A(0.5T_{be}^4 + 0.06T_{ai}^4 + 0.44T_{ae}^4 - T^4). \quad (4)$$

Substitution of equations (3) and (4) into (2) gives

$$T = T_{ne} + \frac{\lambda A}{C} \left[0.25 J_a + \sigma(0.5T_{be}^4 + 0.06T_{ai}^4 + 0.44T_{ae}^4 - T^4) \right] - \lambda(dT/dt). \quad (5)$$

In the present development, we will ignore the last term on the right in equation (5). To perform a complete quantitative development with all terms in equation (5) would necessitate specifying initial conditions for T and an initial height for the sounding. This would introduce the additional problem of nosecone heating, which we would prefer not to consider at the present time. We might further rationalize by saying that rough calculations show the magnitude of the last term in equation (5) to be quite small below approximately 62 kilometers. Above this level, its neglect becomes somewhat more serious; however, if we use

$$T = T_{ne} + \frac{\lambda A}{C} \left[0.25 J_a + \sigma(0.5T_{be}^4 + 0.06T_{ai}^4 + 0.44T_{ae}^4 - T^4) \right] \quad (6)$$

we will at least have a good first order approximation for the temperature of the thermistor when exposed to a convective and radiational environment as given by equations (3) and (4).

Physically, the neglect of the last term in equation (5) implies that the thermistor has come into equilibrium with its radiational and convective environment. As long as the heat transfer environment remains the same, the temperature error will be constant. It is this error which we will compute in the current study using equation (6). In reality, however, the heat transfer environment is changing as the instrument falls through the atmosphere, thus giving a variable temperature error. Consequently, the temperature of the thermistor is not constant, but changing with time during its descent. The last term in equation (5) takes into account the effect of a variable thermistor temperature on the resulting temperature error.

For the thermistor used in the Arcas rocketsonde, many of the terms in equation (6) are fixed constants or known functions of height; among these are λ , C , A and σ . Solar flux will be assumed constant with height in the 20 to 80 km interval. A value of 0.042 cal/cm²/sec will be used. This is 25 per cent larger than the solar constant and is intended to account for atmospheric and terrestrial reflection and scattering.

Values for the effective blackbody radiation temperature of the natural environment above and below the thermistor are obtained by smoothing and extrapolating data given by Aagard (1960). The specification of the effective radiation temperature of the instrument package is rather difficult. It seems reasonable to assume that, because of the large mass of the package, its thermal lag would be extremely large, especially in the upper portion of the height interval under consideration. The values shown in Table II are, therefore, thought to be quite reasonable, even though subjective.

The temperature of the near environment is obtained by taking T_{fe} at a given level and adding to it a correction for compressional and frictional heating. According to Middleton (1953) the temperature rise experienced by a thermometer exposed to high speed airflow will be given by

$$\Delta T = \alpha \frac{v^2}{2c_p} \quad (7)$$

where α is a proportionality constant which is determined experimentally for a particular type of thermometer. Middleton states that this factor usually lies in the range of 0.6 to 0.85. We will arbitrarily use a value of 0.8. The temperature of the near environment will then be given by

$$T_{ne} = T_{fe} + \Delta T = T_{fe} + 0.4 \frac{v^2}{c_p} \quad (8)$$

The ventilation speed is determined from a second degree polynomial fit by root-mean-square techniques to observational data in the height interval 30 to 65 km (approximately) and used for extrapolation down to 20 km and up to 80 km.

Values for the various height dependent parameters are given in Table II.

Equation (5) may be solved for the temperature of the sensing element as a function of height and solar absorptivity. From this, the temperature error, $T - T_{fe}$, may be easily determined. In order to solve this fourth order polynomial in T , an iterative technique was employed where the first assumed value for T is taken as T_{ne} . The Newton-Raphson method was used and found to be convergent. Iteration was continued until the absolute value of the difference between two successive iterates was less than or equal to 0.01°C. The entire process was programmed for the CDC 1604 computer.

The results of the solution of equation (5) are shown in Figure 8. Evaluation of the equilibrium temperature difference between the thermistor and far environment was performed in 3 km increments from 20 km to 80 km and for solar absorptivities of 0.0, 0.05, 0.1, 0.15 and 0.2. Only curves for 0.0, 0.1 and 0.2 are shown in Figure 8; the temperature error associated with the intermediate values can be obtained with sufficient accuracy by linear interpolation.

Several items of interest are apparent in this figure. If we initially stipulate that reasonable accuracy for temperature measurement is $\pm 2^\circ\text{C}$, then we can see that uncorrected temperature data should be "reasonably accurate" up to 57 to 60 km, depending upon the solar absorptivity of the sensor (assuming that it is at least in the interval 0.0 to 0.2). Additionally, only an approximate value for the solar absorptivity is needed since the variation in temperature error with solar absorptivity is fairly small (within $\pm 6^\circ\text{C}$) up to about 70 km. Any attempt at temperature correction above 70 km would be questionable, not only because of the increasing dependence upon an accurate knowledge of the solar absorptivity, but also because of the increasing importance of the term which was neglected in equation (5).

The solar absorptivity of the white Krylon coated thermistor is thought to be in the interval 0.1 to 0.2. If we assume that, due to the swinging motion of the parachute, the sensing element will, periodically, be exposed to direct sunlight followed by shade, then the average solar flux reaching the thermistor would undoubtedly be less than the $0.042 \text{ cal/cm}^2/\text{sec}$ which was used in performing the calculations. We can account for this by considering an "effective solar absorptivity" which is somewhat smaller than the true value. A reasonable choice would seem to be 0.1 for daytime soundings. For nighttime soundings the choice should obviously be 0.0. Table III shows the amount which should be added to the observed temperature (to the nearest degree) in order to obtain a temperature as previously described. Having applied these corrections to observed temperature data, an accuracy of $\pm 0.5^\circ\text{C}$ should be achieved.

ADDITIONAL SOURCES OF ERROR

During the ascent of the rocket through the atmosphere, the nosecone is subjected to extreme heating effects as a result of adiabatic compression and friction. This would be particularly true of the forward portion of the nosecone which encloses the temperature sensor. The thermistor would thus be exposed to an environment which is radiating at a fairly high temperature in the infrared. At near zero ventilation speed and low pressure, the thermistor would come into radiational equilibrium rather than convective equilibrium with its environment.

Temperature signals are sent by the instrument during ascent; however, the sensitivity of the signal at high temperature is extremely poor. The signal is definitely associated with a temperature which is higher than surface ambient, and in most cases approaches the reference signal level (corresponding to a thermistor of zero resistance). In the numerical development here an arbitrary value of $+50^\circ\text{C}$ will be used as the temperature

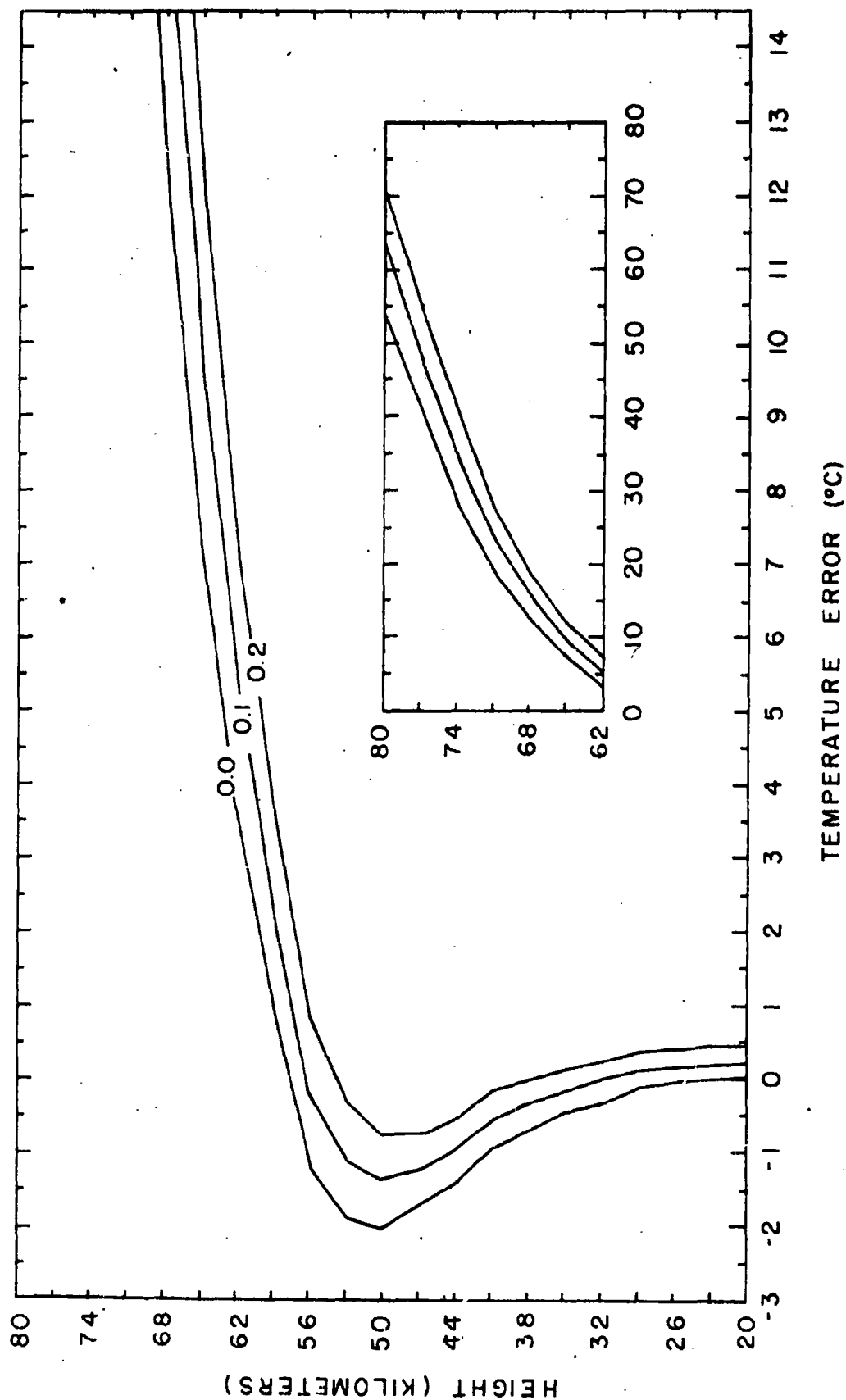


Figure 8.

COMBINED COMPRESSORAL HEATING AND RADIATIVE TEMPERATURE
ERROR OF THE ARCAS ROCKETSONDE THERMISTOR

of the thermistor immediately prior to nosecone separation. This is considered to be a conservative estimate.

The problem in its simplest form is to derive the temperature-height relationship which would be indicated by the thermistor as it approaches convective equilibrium with the atmospheric environment after nosecone separation. A considerably more complicated, but more complete, statement of the problem would include, in addition to convective equilibrium, radiational equilibrium, compressional heating effects, and internal heating effects.

Considering only compressional heating and nosecone heating, we would expect an observed temperature record to look similar to that shown in Figure 9. The thermistor is exposed to a standard atmosphere environment at about 87 km. The temperature of the thermistor is initially 50°C. Compressional heating initially causes some slight increase in the temperature, but soon the fall speed has decreased such that the thermistor temperature begins to approach that of the environment. At about 62 km the thermistor finally reaches and crosses over the environmental curve. Additional calculations have shown that this cross-over point is about 62 km \pm 2 km regardless of the initial height of the sounding.

An additional source of error is a result of the power dissipation in the thermistor due to the measuring current. Again turning to Ballard's experimental work for values of temperature change per unit power and using a typical instrument for current measurement, the values of Figure 10 were computed. This effect is referred to as internal heating.

APPLICATIONS AND CONCLUSIONS

From the above discussion, it is apparent that the measurement of high-altitude winds and temperatures has been accomplished with relatively simple systems. However, even these systems have involved the introduction of some complicated corrective calculations and limitations which can lead to a dilemma. Consider Figure 2. Of the sensors included, only the nylon chaff offers an effective wind sensing system above 200,000 feet, but fall velocity and dispersion effects limit its practical application below about 150,000 feet. Each of the sensors offer certain advantages over particular altitude ranges while no single sensor provides completely satisfactory measurements over the altitude range of interest. The problem of temperature measurements also involves compromise and correction.

Nonetheless, significant data can be, and have been, gathered with such systems with increasing efficiency and regularity on a synoptic basis. Although, thus far, the major effort has been toward the basic wind and temperature measurements, applications of these measurements will naturally follow. Speed-of-sound and density calculations based on Meteorological Rocket Network data have been accomplished for White Sands Missile Range, Fort Greely, Alaska and Fort Churchill, Canada. Figure 11 is an example of typical meteorological rocket data profiles as they appear in the Meteorological Rocket Network publications. It will be noted that radiosonde

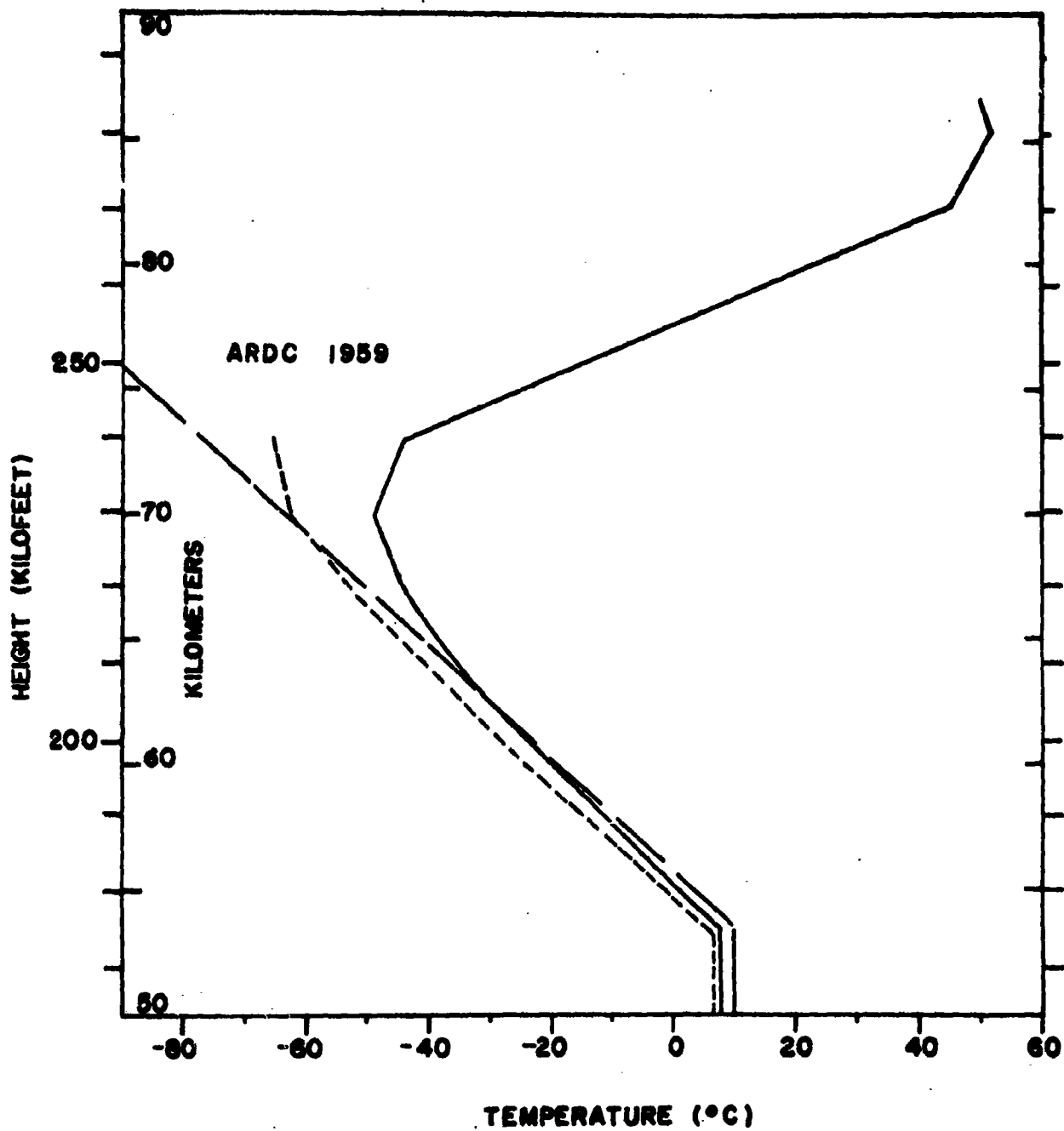


Figure 9. Indicated temperature (solid line) and temperature corrected for compressional heating (dashed line) for the Arcas rocketsonde thermistor.

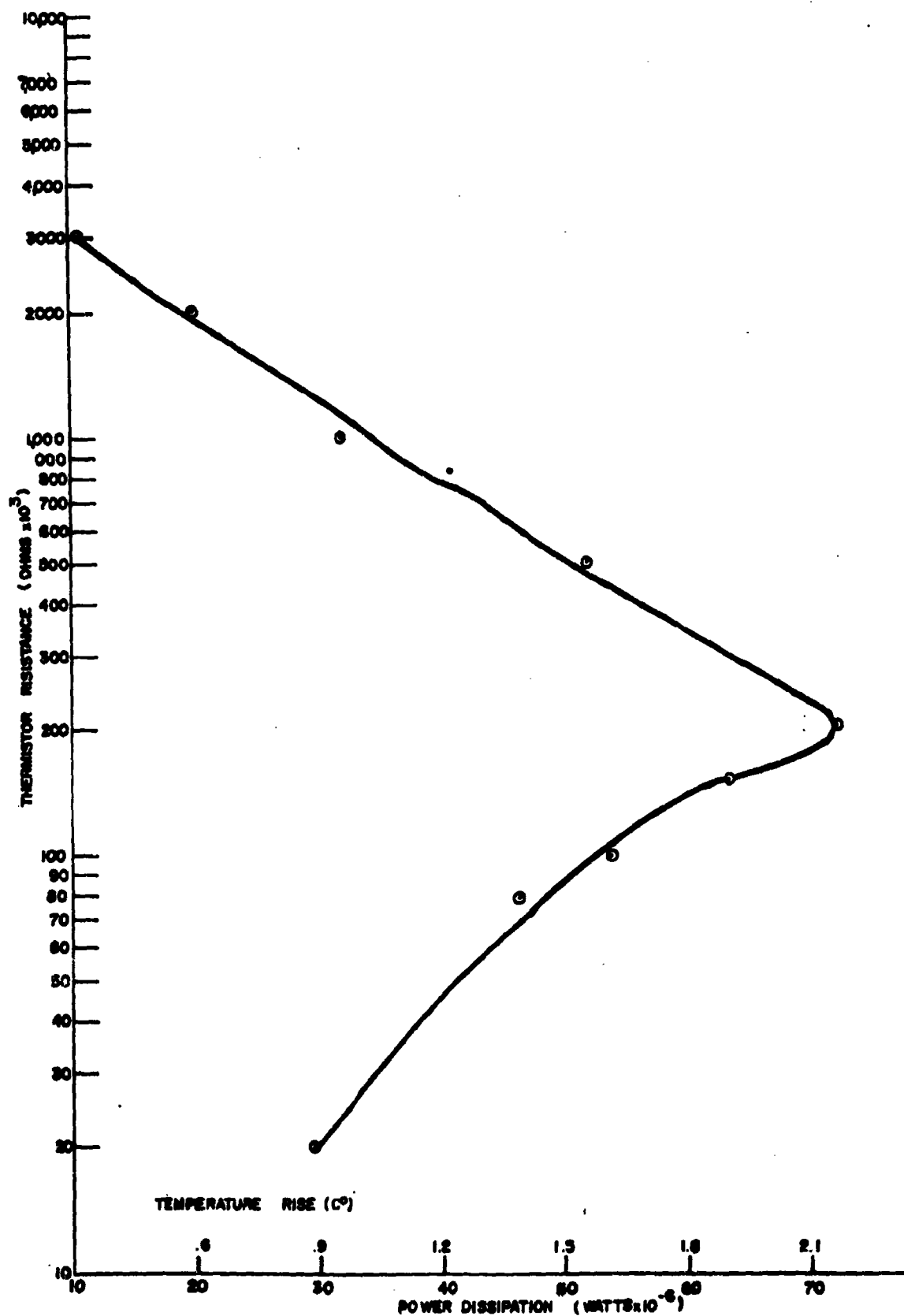


Figure 10. Power dissipation of Gamma and associated temperature rise at 8mm pressure with Krylon coated bead thermistor. 25

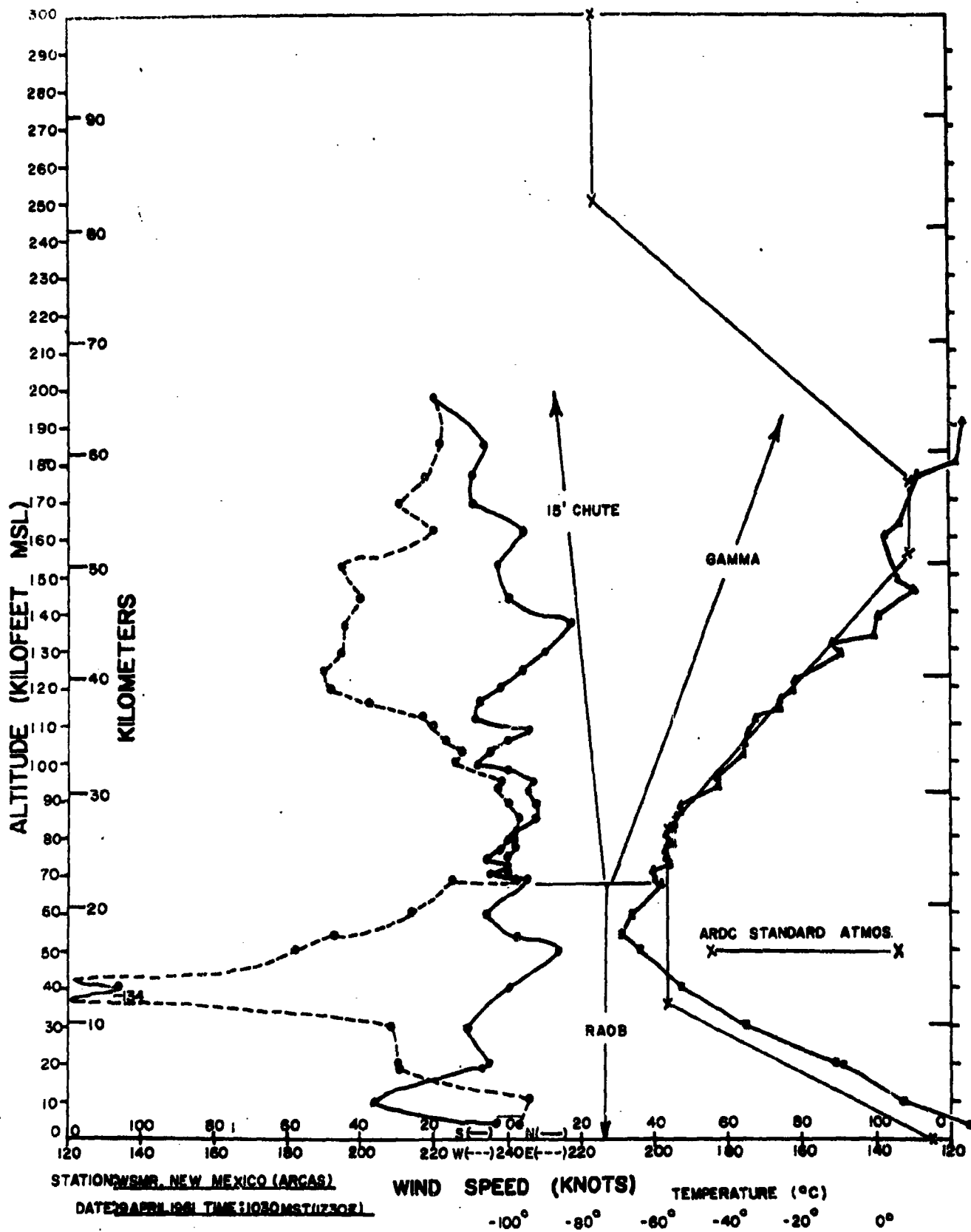


Figure 11. Typical rocketsonde - Raob profile

data were incorporated with the rocket data to obtain a continuous profile starting from the surface. The temperature profile of Figure 11 was applied in the computations of the speed of sound and the density to arrive at the structures in Figure 12. Note that the speed of sound is based only on the temperature structure, and the atmosphere motions (wind) may be incorporated for a directional distribution of the speed of sound.

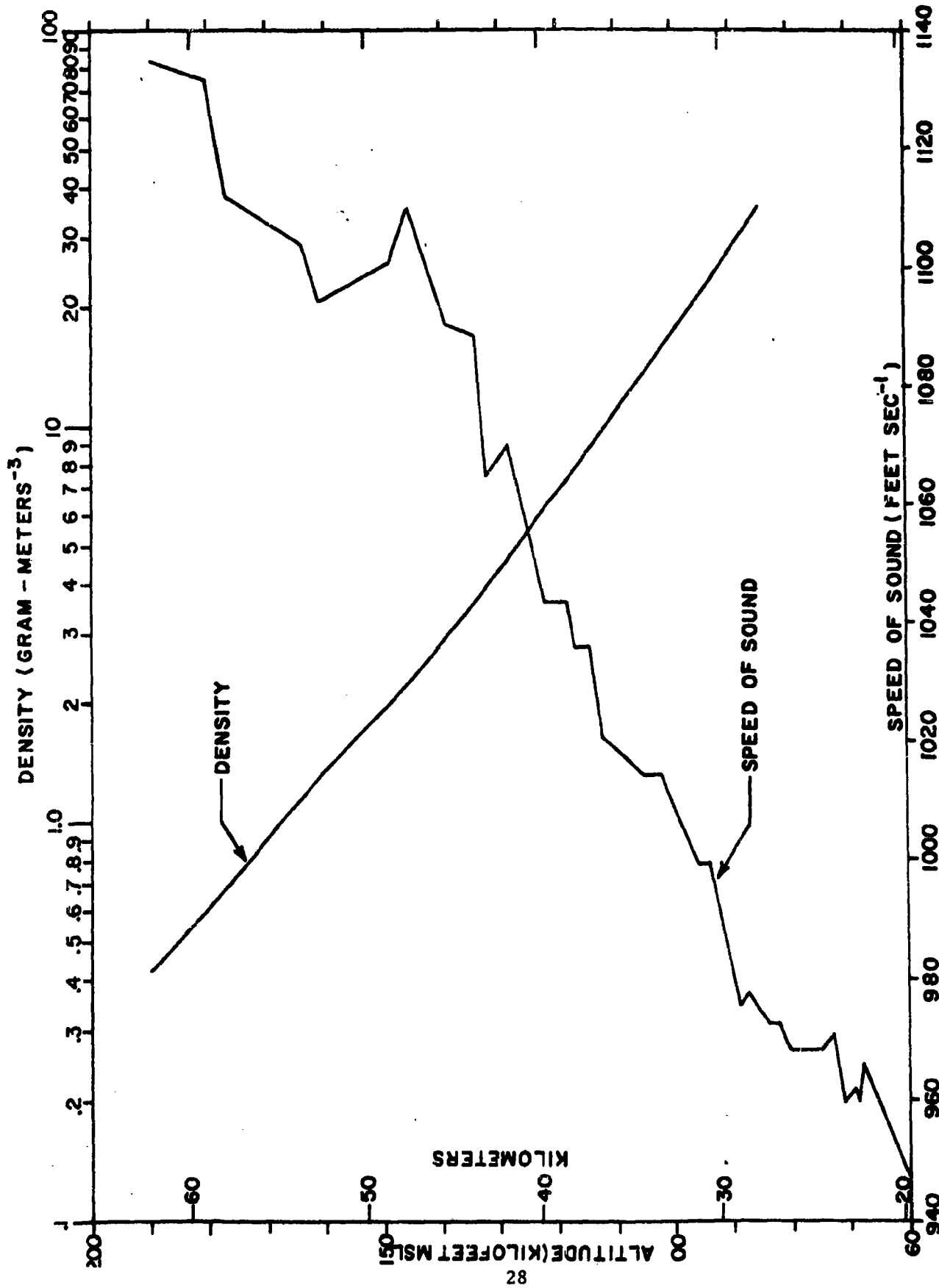


Figure 12. Density and speed of sound profiles derived from rocketsonde data.

REFERENCES

- Aagard, Roger L., 1960: Measurements of Infrared Radiation Divergence in the Atmosphere with the Double-Radiometer and the Black Ball, Jour. of Met., 17(3), pp. 311-318.
- Ballard, H. N., 1961, "Response Time of and Effects of Radiations on the VECO Bead Thermistor," ISA-AMS, Sept. 11-15, 1961, Los Angeles, Preprint 167-LA-61.
- Barr, W. C., "Theoretical Evaluation of Cylindrical Chaff as a Wind Sensor at High Altitudes," TR 2138, U. S. Army Signal Research and Development Laboratory, AD 241876.
- Beyers, N. J., 1960, "Preliminary Radar Performance Data on Passive Rocket-Borne Wind Sensors," IRE-Transactions on Military Electronics, Vol MIL-4, No 2-3, 230-233.
- Clark, G. Q., 1961, "Development of a Rocket Telemetry Package for the Meteorological Rocket Network," Initiation of the Meteorological Rocket Network, IRIG Document No 105-60, Revised August 1961, AD 246950.
- Eckert, E. R. G., and R. M. Drake, Jr., 1959, "Heat and Mass Transfer," McGraw-Hill Book Company, Inc., New York, 530 pp.
- Jenkins, K. R., 1962, "Empirical Comparisons of Meteorological Rocket Wind Sensors," Journal of Applied Meteorology Vol 1, No 2, June 1962.
- Jenkins, K. R., W. L. Webb, and G. Q. Clark, 1960, "Rocket Soundings of High Atmosphere Meteorological Parameters," PGMIL Trans. (Inst. Radio Eng.), MIL-4, No 2-3, 238-243.
- Lally, V. E. and R. Leviton, 1958, "Accuracy of Wind Determination from the Track of a Falling Object," U. S. Air Force Cambridge Research Center, Air Force Surveys in Geophysics, No 93, AD 146858.
- Middleton, W. E. Knowles and A. F. Spilhaus, 1953: Meteorological Instruments, 3rd Ed., Rev., Univ. of Toronto Press, Toronto, Canada, 286 pp.
- Rapp, R. R., 1960, "The Accuracy of Wind Derived by the Radar Tracking of Chaff at High Altitudes," Journal of Meteorology, Vol 17, No 5.
- Wagner, N. K., 1961, "Theoretical Time Constant and Radiation Error of a Rocketsonde Thermistor, Journal of Meteorology, Vol 18, No. 5.
- Webb, W. L., W. E. Hubert, R. L. Miller, and J. F. Spurling, 1961, "The First Meteorological Rocket Network," Bull. Amer. Meteor. Soc., 42, 482-494.

N O T I C E S

Approval. Technical Report SELWS-M-4 has been reviewed and approved for publication:



CLARENCE E. MORRISON
Lt Col., Signal Corps
Chief, Missile Meteorology Division



WILLIS L. WEBB
Chief Scientist
Missile Meteorology Division

Distribution. This report has been distributed in accordance with SELWS-M List Nr. 2. Initial printing 129 copies.

ASTIA Availability. Qualified requesters may obtain copies of this report from:

Armed Services
Technical Information Agency
Arlington Hall Station
ATTN: TIPCR
Arlington 12, Virginia


HEADQUARTERS
U. S. ARMY ELECTRONICS RESEARCH AND DEVELOPMENT ACTIVITY
WHITE SANDS MISSILE RANGE
NEW MEXICO

October 1962

1. Technical Report SELWS-M-4 has been prepared under the supervision of the Missile Meteorology Division and is published for the information and guidance of all concerned.

2. Suggestions or criticisms relative to the form, contents, purpose, or use of this publication should be referred to the Commanding Officer, U. S. Army Electronics Research and Development Activity, ATTN: Chief, Missile Meteorology Division, White Sands Missile Range, New Mexico.

FOR THE COMMANDER:


L. W. ALBRIGHT
Major, AGC
Adjutant

AC ARMED SERVICES Research and Development Activity Missile Technology Division, White Sands Missile Range, New Mexico PERFORMANCE CHARACTERISTICS OF METEOROLOGICAL ROCKET WIND AND TEMPERATURE SENSORS, by Norman J. Beyers, Otto W. Thiele, and N. K. Wagner, Technical Report SEJMS M-4 October 1962, 31 pp incl illus. UNCLASSIFIED Report	UNCLASSIFIED 1. Atmosphere 2. Meteorology 3. Temperature 4. Pressure 5. Wind 6. Density 7. Speed of Sound Qualified requesters may obtain copies of this report from: Armed Services Technical Information Agency Arlington Hall Station ATTN: TIPCR Arlington 12, Virginia	ACCESSION NR	UNCLASSIFIED 1. Atmosphere 2. Meteorology 3. Temperature 4. Pressure 5. Wind 6. Density 7. Speed of Sound Qualified requesters may obtain copies of this report from: Armed Services Technical Information Agency Arlington Hall Station ATTN: TIPCR Arlington 12, Virginia	AD ARMED SERVICES Research and Development Activity Missile Technology Division, White Sands Missile Range, New Mexico PERFORMANCE CHARACTERISTICS OF METEOROLOGICAL ROCKET WIND AND TEMPERATURE SENSORS, by Norman J. Beyers, Otto W. Thiele, and N. K. Wagner, Technical Report SEJMS M-4 October 1962, 31 pp incl illus. UNCLASSIFIED Report	UNCLASSIFIED 1. Atmosphere 2. Meteorology 3. Temperature 4. Pressure 5. Wind 6. Density 7. Speed of Sound Qualified requesters may obtain copies of this report from: Armed Services Technical Information Agency Arlington Hall Station ATTN: TIPCR Arlington 12, Virginia	ACCESSION NR
AC ARMED SERVICES Research and Development Activity Missile Technology Division, White Sands Missile Range, New Mexico PERFORMANCE CHARACTERISTICS OF METEOROLOGICAL ROCKET WIND AND TEMPERATURE SENSORS, by Norman J. Beyers, Otto W. Thiele, and N. K. Wagner, Technical Report SEJMS M-4 October 1962, 31 pp incl illus. UNCLASSIFIED Report	UNCLASSIFIED 1. Atmosphere 2. Meteorology 3. Temperature 4. Pressure 5. Wind 6. Density 7. Speed of Sound Qualified requesters may obtain copies of this report from: Armed Services Technical Information Agency Arlington Hall Station ATTN: TIPCR Arlington 12, Virginia	ACCESSION NR	UNCLASSIFIED 1. Atmosphere 2. Meteorology 3. Temperature 4. Pressure 5. Wind 6. Density 7. Speed of Sound Qualified requesters may obtain copies of this report from: Armed Services Technical Information Agency Arlington Hall Station ATTN: TIPCR Arlington 12, Virginia	AD ARMED SERVICES Research and Development Activity Missile Technology Division, White Sands Missile Range, New Mexico PERFORMANCE CHARACTERISTICS OF METEOROLOGICAL ROCKET WIND AND TEMPERATURE SENSORS, by Norman J. Beyers, Otto W. Thiele, and N. K. Wagner, Technical Report SEJMS M-4 October 1962, 31 pp incl illus. UNCLASSIFIED Report	UNCLASSIFIED 1. Atmosphere 2. Meteorology 3. Temperature 4. Pressure 5. Wind 6. Density 7. Speed of Sound Qualified requesters may obtain copies of this report from: Armed Services Technical Information Agency Arlington Hall Station ATTN: TIPCR Arlington 12, Virginia	ACCESSION NR